214
4-23-76

Dr-53

Y-2016

GAMMA SPECTRA OF THE 234, 235, AND 238 URANIUM ISOTOPES

Alden King

April 1976

UNION CARBIDE

OAK RIDGE Y-12 PLANT
OAK RIDGE, TENNESSEE

prepared for the **U.S. ENERGY RESEARCH AND DEVELOPMENT ADMINISTRATION**
under **U.S. GOVERNMENT** *Contract W-7405 eng 26*

DISCLAIMER

Reference to a company or product name does not imply approval or recommendation of the product by Union Carbide Corporation or the U.S. Energy Research and Development Administration to the exclusion of others that may meet specifications.

Printed in the United States of America. Available from
National Technical Information Service
U.S. Department of Commerce
5285 Port Royal Road, Springfield, Virginia 22161
Price: Printed Copy $4.00; Microfiche $2.25

Date of Issue: **April 27, 1976**
Distribution Category: **UC-41**

Report Number: **Y-2016**

GAMMA SPECTRA OF THE 234, 235, AND 238 URANIUM ISOTOPES

Alden King

Radiation Safety Department
Y-12 Technical Division

Adapted from a thesis that was submitted to The University of Tennessee in partial fulfillment of the requirements for the degree Master of Science.

Oak Ridge Y-12 Plant
P. O. Box Y, Oak Ridge, Tennessee 37830

Prepared for the US Energy Research
and Development Administration
Under US Government Contract W-7405-eng-26

ABSTRACT

Eight sources of uranium of varying ^{235}U enrichment were used to collect detailed gamma-ray spectra with a GeLi detector over the energy range from 50 to 250 keV. The characteristic X rays of thorium and uranium were identified. Included in the spectra were gamma rays present in the decay of the 234, 235, and 238 uranium isotopes. The efficiency of the detector was determined and used to calculate both conversion coefficients for the ^{234}U decay gamma rays and the abundance of the various X rays and gamma rays relative to their parent uranium isotope. It was anticipated that this information could be reasonably applied to in vivo monitoring for uranium isotopes.

CONTENTS

SUMMARY

Gamma spectra were collected and calculated for various uranium sources of known isotopic distribution. The data were tabulated using existing computer programs which located and totaled each peak. Plots were also made, using existing computer programs. The gamma-ray peaks at 10.4, 237 and 249 keV are present in all the spectra collected, including the background run. Thus, they were reasonably attributed to background radiation. The low-energy gamma rays from ^{238}U (48 keV) and ^{236}U (49.8 keV) were easily converted to electrons and readily absorbed in the excitation of X rays. Those quanta which remained after these processes were not detected in the relatively short count times of this work. As a check, the collected and calculated data of this work were used to calculate an efficiency for the detector used. Since the efficiency of the detector was not known, it was tabulated via a computer program using the Newton-Coates method of numerical integration. As a rule, the experimentally derived efficiency was in agreement with the numerically integrated one.

It is anticipated that the results of this work could be applied to in vivo monitoring for the various isotopes of uranium. It has been demonstrated in this work that the 48-keV gamma ray from ^{238}U and the 49.8-keV gamma ray from ^{236}U could not be applied in in vivo monitoring. It is felt, however, that, given solid-state detection equipment and sufficiently long count times, the 53.3 and 120.9-keV photons could, at some future time, be considered feasible for use in in vivo monitoring for ^{234}U.

INTRODUCTION

As long as man is required to work with hazardous materials, there will exist a need for a means of determining the extent of his exposure to such materials. In vivo monitoring is a means of measuring the internal exposure of an individual to radioactive isotopes, using gamma-ray spectrometry instrumentation and techniques. This study resulted, in part, from a desire for a more detailed knowledge of the gamma-ray spectra arising from the 234, 235, and 238 uranium isotopes which could be applied to in vivo counting for these isotopes. Present in vivo monitoring apparatus generally consists of a sodium iodide crystal gamma-ray spectrometer with an associated data evaluation system. Large-volume sodium iodide crystals are used because of the great sensitivity which they afford, but they lack resolution, particularly at low photon energies.

Due to a desire for detailed gamma spectra, this work[a] was conducted with a germanium, lithium-drifted (GeLi), semiconductor detector to take advantage of its high resolution. In order to detect gamma-ray photons, the GeLi detector was connected to a pulser, bias amplifier, preamplifier, and a multichannel analyzer. The pulse generator was incorporated into the system to facilitate calibration. Although having only 10% of the efficiency of equivalent NaI detectors, the energy resolution of semiconductor detectors can be as much as ten times better than the scintillation detector. This improvement allows better separation and identification of the individual photon peaks.

(a) Performed at the Oak Ridge Y-12 Plant which is operated by the Union Carbide Corporation's Nuclear Division for the US Energy Research and Development Administration.

GAMMA SPECTRA OF THREE URANIUM ISOTOPES

THE DETECTOR

Detector Interaction Process

When a photon enters a GeLi detector it creates electron-hole pairs by losing energy at the rate of 2.98 electron volts per electron-hole pair produced. This interaction produces a small current which is detected and amplified by the electronics of the system. The dominant mode of interaction, which is discussed here, is the photoelectric effect.

The interaction of a photon with a bound atomic electron leading to the complete absorption of the photon is termed the "photoelectric effect". This effect predominates at low incident photon energies. In the photoelectric interaction, the incident photon gives up all its energy to a bound electron. The electron then uses part of that energy to overcome its binding potential and the rest becomes electron kinetic energy. Before the photoelectric interaction can take place, the photon energy must exceed the binding energy of the electron. The binding energy of the electron subsequently appears in the form of characteristic X rays and Auger electrons resulting from the filling of the shell vacancy created by the photoelectron. About 80% of the photoelectric interactions take place in the K shell of an atom and most of the remaining 20% occur in the L shell. The probability of a photoelectric interaction occurring is highest when the incident photon energy is just higher than that required for the emission of a particular spectral series. K-shell electron vacancies give rise to X radiation that is characteristic of the K shell. Similarly, L-shell vacancies give rise to X radiation characteristic of the L shell. Each spectral series, whether K, L, or M, will contain alpha (α), beta (β), and gamma (γ) lines when the vacancies are filled by the respective energy shells immediately higher than the vacancy shell. Subshell interactions give rise to $\alpha 1$, $\alpha 2$, $\beta 1$, $\beta 2$, and $\beta 3$ spectral lines. Martin, et al (1970) list examples (Table 1) of the predominant K-shell characteristic X rays. The appearance of the spectral peaks varies with the mass of the element which emits the X ray. This variance is illustrated in Figure 1. In all cases, the relative intensities are on the order of $K\alpha 1$ (100%), $K\alpha 2$ (50%), and $K\beta 1$ (25%). Lederer, et al (1968) list the relative K-shell X-ray intensities of thorium as $K\alpha 1$ (100%), $K\alpha 2$ (56%), $K\beta 1$ (38%), and $K\beta 2$ (13%).

Detector Apparatus

The apparatus used in this work consisted of a lithium-drifted germanium (GeLi) semiconductor detector electrically attached to a pulse height analyzer through a bias amplifier, preamplifier, and amplifier. A pulse generator was attached to the input of the preamplifier to permit calibration of the system. Figure 2 is a block diagram of the electronic equipment used. The detector was a 10% coaxial GeLi detector having an effective interaction volume of 55 cubic centimeters. Before striking the interaction volume, the photons passed through a 0.5-mm aluminum window, a 1.0-mm thickness of Teflon, and a 1.2-mm germanium dead

Table 1

PREDOMINANT K-SHELL X RAYS AND THE SHELL FROM WHICH THE ELECTRON VACANCIES ARE FILLED

X Ray	Shell Decaying
$K\alpha 1$	L-III
$K\alpha 2$	L-II
$K\beta 1$	M-III
$K\beta 2$	N-III
$K\beta 3$	M-II
$K\beta 4$	N-II
$K\beta 5$	M-IV

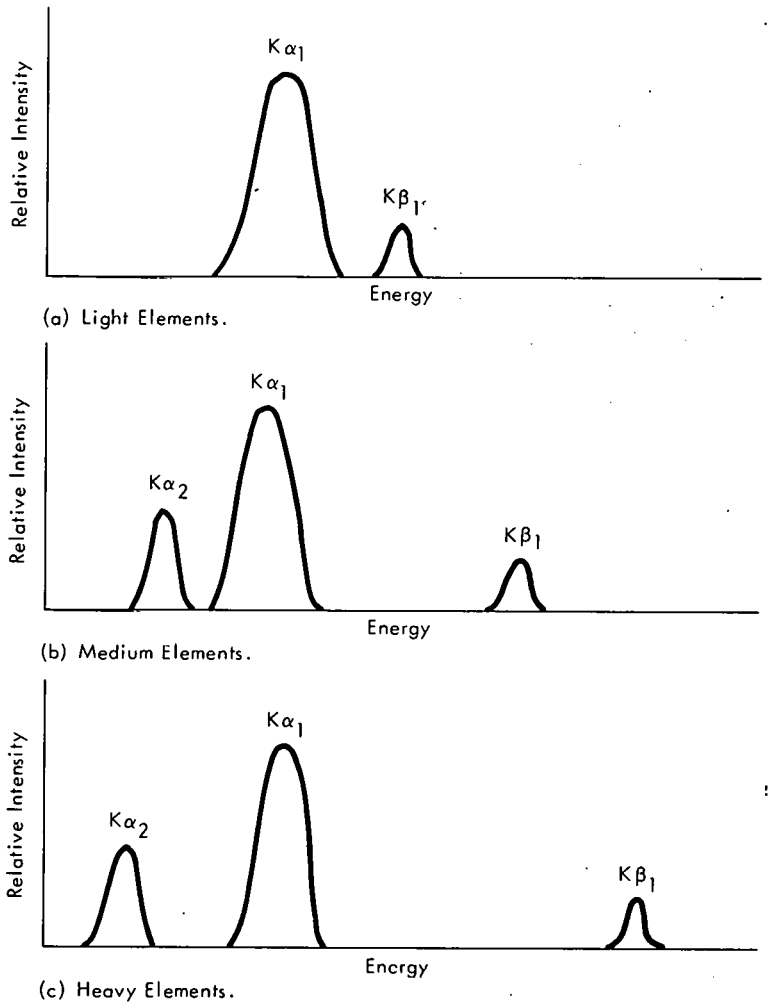

Figure 1. CHARACTERISTIC K-SHELL X RAYS AS THEY APPEAR WHEN RESULTING FROM LIGHT ELEMENTS, MEDIUM ELEMENTS, AND HEAVY ELEMENTS.

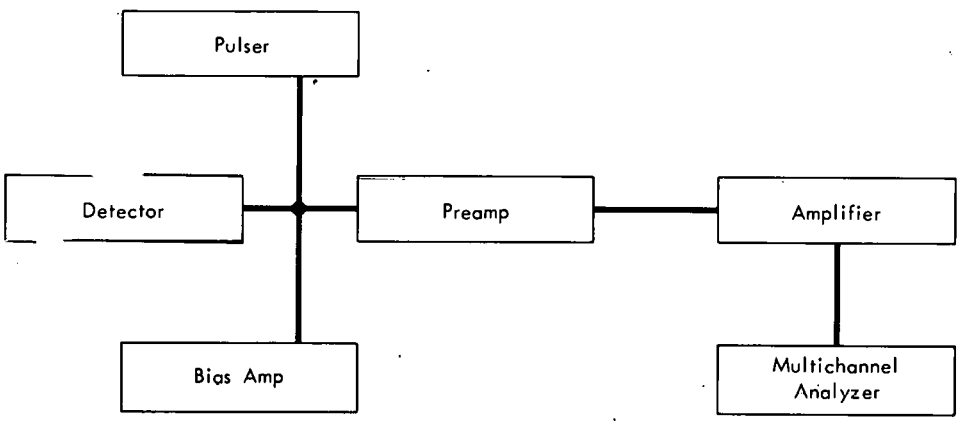

Figure 2. BLOCK DIAGRAM SHOWING THE ELECTRONIC EQUIPMENT USED IN THE STUDY.

layer. The active volume of the detector was located 5.0 mm from the aluminum window. It was this aluminum window which filtered out the low-energy characteristic L X-ray spectra. The pulse height analyzer was a Nuclear Data Model 2400 multichannel analyzer operating in 1024 channels. The system was electronically calibrated to 0.25 keV per channel, using an ORTEC Model 448 pulser. The pulse generator was normalized to the 121.9-keV gamma-ray photon arising from the decay of cobalt 57. Calibration data arising from this method are listed in Table 2. A plot of these calibration data with energy versus channel is given in Figure 3. The slope of this line was found to be 0.25 keV per channel. In actuality, the data were treated in an existing computer program which applied a least-squares fit to arrive at the slope.

Table 2

CALIBRATION DATA RESULTING FROM USE OF THE PULSER

Energy (keV)	Channel Number
20	81
60	241
121.9	488
160	639
200	801

Detector Efficiency

A 10% semiconductor detector is, by definition, one which has one-tenth the efficiency of a 3 x 3-inch NaI scintillation detector measured at 1.33 MeV, with a source-to-detector distance of 25 cm. For the purposes of this study, several efficiencies should be defined:

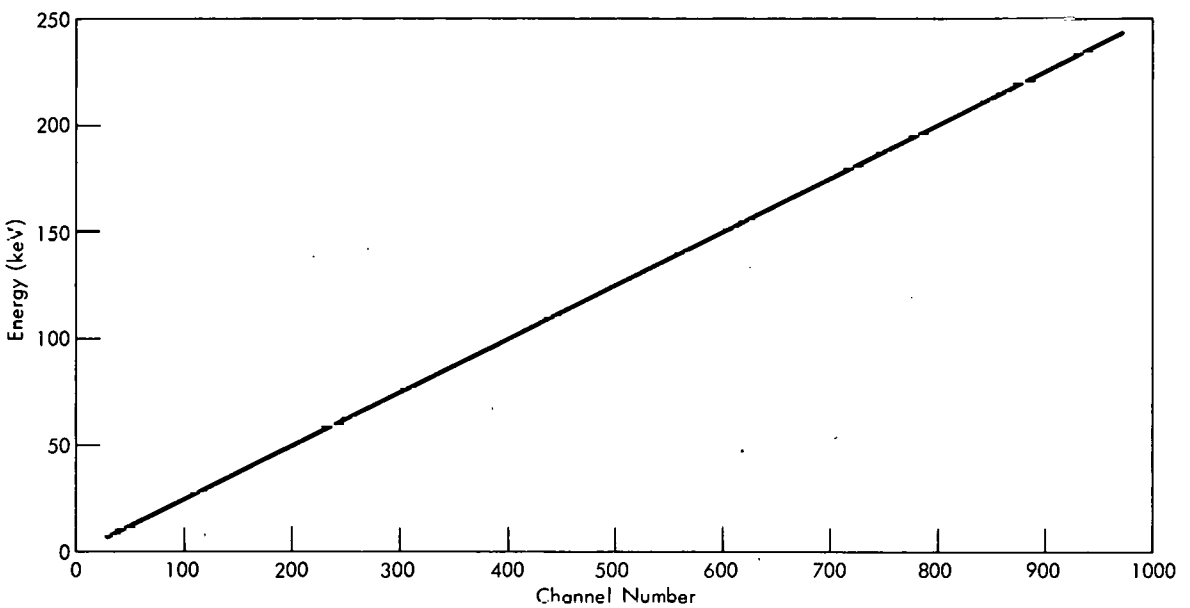

Figure 3. CALIBRATION PLOT OF ENERGY VERSUS CHANNEL NUMBER.

Photopeak Efficiency - The photopeak efficiency (ϵ_p) is the probability that a photon entering the detector will produce a pulse in the corresponding photopeak. If (I) is equal to the quantity of radiation passing through the detector and (I_0) is equal to the quantity of incident radiation, the two are related according to the formula:

$$I = I_o e^{-\mu_m \rho t} ,$$

where (μm) is the photoelectric mass absorption coefficient of the detector medium, (ρ) is the density of the detector material, and (t) is the detector thickness. The photopeak efficiency is then equal to the ratio of the radiation absorbed in the detector to the radiation incident upon the detector. Thus:

$$\epsilon_p = \frac{\text{Absorbed Radiation}}{\text{Incident Radiation}} = \frac{I_o - I}{I_o} = \frac{I_o - I_o e^{-\mu_m \rho t}}{I_o} ,$$

and:

$$\epsilon_p = 1 - e^{-\mu_m \rho t} .$$

This final expression is a good approximation for the photopeak efficiency when, as in this work, the photoelectric interaction predominates. As the incident photon energy increases, losses due to Compton scattering increase and bring about an additional decrease in the photopeak efficiency.

Geometric Efficiency - Geometric efficiency is the probability that a photon from a particular source will strike the detector. For point sources having a radius much smaller than the source-to-detector distance, the geometric efficiency is the ratio of the visible area of the detector to the surface area of the sphere of radius equal to the source-to-detector distance. The radioactive areas on the sources used in this work were attached directly to the detector window in such a manner that they completely covered the active region of the detector.

Absolute Efficiency - The absolute efficiency of a detector can be described as the product of the photopeak efficiency and the geometric efficiency. Because of the short source-to-detector distance and the fact that disc sources rather than point sources were used, this discussion only approximates the absolute efficiency. In reality, the calculation is more complex. Vegors Jr., et al (1958) describe a source and detector arrangement comparable to that used in this work. They reduced the calculation of the detection efficiency for disc sources as being the following integral:

$$\text{Eff} = \frac{1}{\pi R^2} \int_0^R x\,dx \int_{-\pi/2}^{\pi/2} d\phi \left\{ \int_0^{\tan^{-1}\left(\frac{-x\sin\phi + \sqrt{x^2\sin^2\phi - (x^2 - r_o^2)}}{h_o + t_o} \right)} \left[1 - e^{-\tau(E)\, t_o/\cos\theta} \right] \sin\theta\, d\theta \right. \quad +$$

$$\int_{\tan^{-1}\left(\frac{-x\sin\phi+\sqrt{x^2\sin^2\phi-\left(x^2-r_o^2\right)}}{h_o}\right)}^{\tan^{-1}\left(\frac{-x\sin\phi+\sqrt{x^2\sin^2\phi-\left(x^2-r_o^2\right)}}{h_o+t_o}\right)} \left[1-e^{-\tau(E)\left(\frac{-x\sin\theta+\sqrt{x^2\sin^2\psi-\left(x^2-r_o^2\right)}}{\sin\theta}-\frac{h_o}{\cos\theta}\right)}\right]\sin\theta\,d\theta$$

where $\tau(E)$ is the linear absorption coefficient of the detector and the geometric parameters involved are defined in Figure 4. Theoretical detector efficiencies were calculated for the apparatus used in this work according to this integral by the Newton-Coates five-point numerical integration method. A modification of the computer program written for this purpose by Van Hull (1975) was used to perform the numerical integration and is shown in Appendix A. The results of this program are listed in Table 3 and plotted in Figure 5. The appearance of this efficiency plot when corrected for the absorbers in the detector is shown is Figure 6.

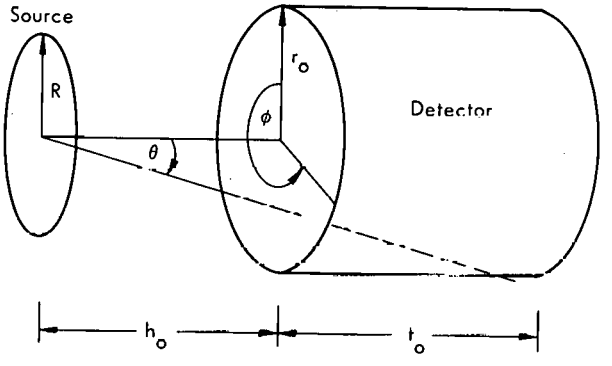

Figure 4. SOURCE-DETECTOR GEOMETRY.

Table 3

THEORETICAL DETECTOR EFFICIENCY RESULTING FROM THE NEWTON-COATES NUMERICAL INTEGRATION

Photon Energy (keV)	Theoretical Efficiency
53	0.270
63	0.266
90	0.246
93	0.243
105	0.228
109	0.222
121	0.202
143	0.162
163	0.129
186	0.098
195	0.089
202	0.083
205	0.080

THE SOURCE

Source Theory and Calculations

It was the objective of this work to collect and identify detailed gamma-ray spectra from uranium sources of varied enrichment and

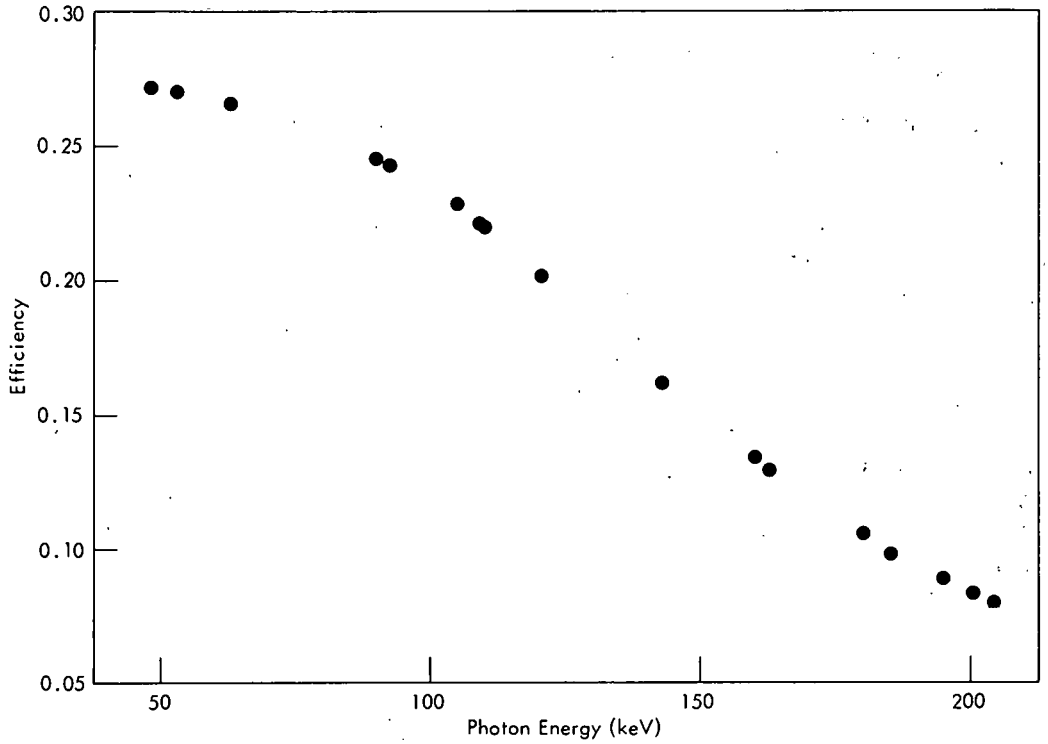

Figure 5. THEORETICAL EFFICIENCY VERSUS INCIDENT PHOTON ENERGY.

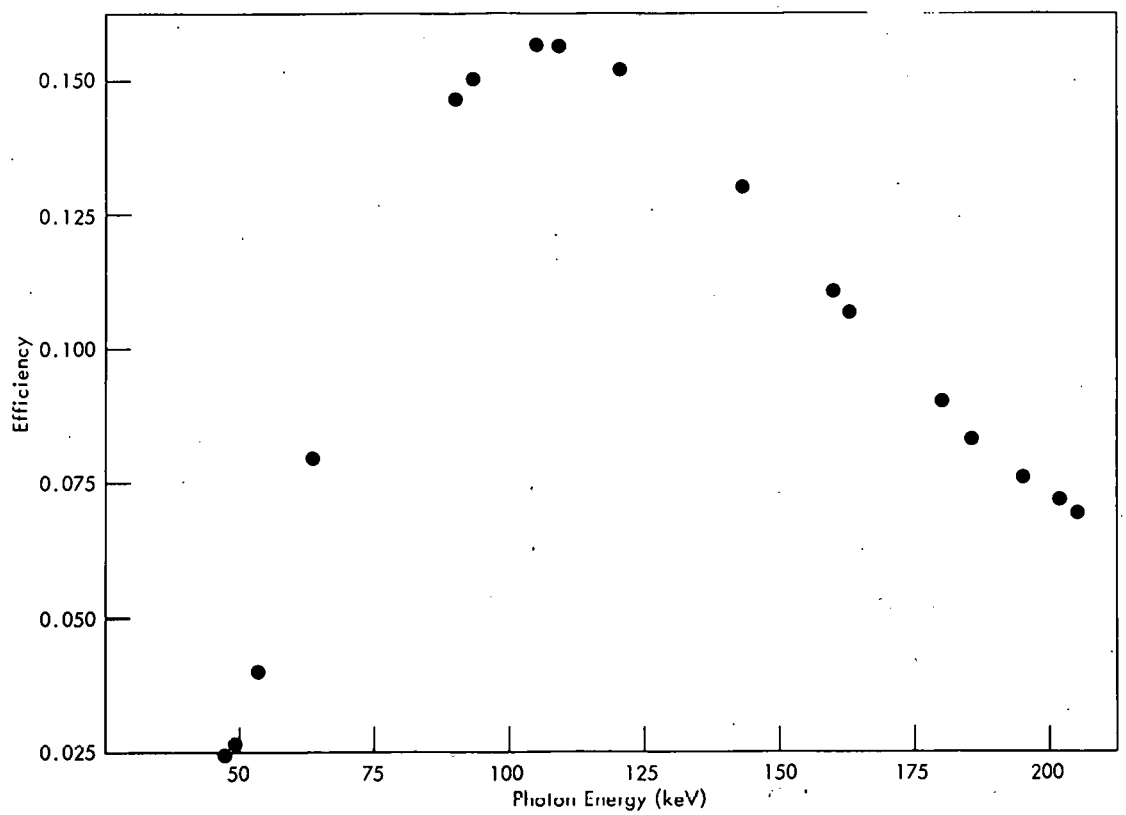

Figure 6. THEORETICAL EFFICIENCY CORRECTED FOR ABSORBERS.

known isotopic distribution. The sources used were of two types: Type 1 sources were metal discs, 49.2 mm in diameter, which had from three to eight milligrams of uranium electroplated onto their surfaces.(b) The plated area had a diameter of 38.1 mm. Type 2 sources were high-purity oxides of uranium.(c) These oxides were encapsulated in a small nylon sample vial.

The isotopic distribution of these sources revealed the presence of the 234, 235, 236, and 238 isotopes of uranium. Accordingly, these were the isotopes considered in computing a theoretical gamma and X-ray decay flux.

Uranium 234 is a high-specific-activity (6198 nCi/mg) alpha emitter. It is present in natural uranium and is concentrated along with ^{235}U in most enriching processes. More than 90% of the internal exposure hazard associated with enriched uranium can be attributed to the 234 isotope because of its relatively high specific activity. This isotope decays 72% of the time to the ground state of ^{230}Th, thus emitting no gamma rays. Approximately 28% of the time, the decay is to an excited state which emits a 53.3-keV gamma ray that is highly absorbed. Uranium-234 decay goes 0.35% of the time to an excited state which decays by emitting a 120.9-keV gamma ray. This 120.9-keV gamma emission also goes to the 53.3-keV level. There are higher-energy gamma rays associated with ^{234}U, but their intensity is so small that they are of no interest in in vivo spectrometry.

Uranium-235 decays by alpha emission. Only 4.6% of the time does this alpha decay go directly to the ground state of ^{231}Th. For the most part, ^{235}U decays to excited states in ^{231}Th, which then emit detectable gamma radiation. Kroger (1972) lists the ^{235}U gamma-ray photons, as given in Table 4. These data are generally in agreement with those reported by Lederer, et al (1968) and Teoh, et al (1974). Photons of energy equal to 192 keV were also reported by Vorob'ev, et al (1960), following gamma-ray coincidence studies. (The specific activity of ^{235}U is 2.145 nCi/mg.)

Table 4

GAMMA-RAY INTENSITIES ARISING IN THE DECAY OF ^{235}U

Energy (keV)	Intensity (%)
109	1.5
143	9.7
163	4.6
183	0.46
186	54.0
195	0.65
202	1.05
205	4.9

Uranium-236 and uranium-238 alpha decay directly to the ground state most of the time. When they do, no gamma rays are produced. Uranium-236 decays to the ground state of ^{232}Th 74% of the time; 26% of the time it decays to an excited state which emits a 49.8-keV gamma ray. Uranium-238 alpha decays 77% of the time to the ground state of ^{234}Th; 23% of the time it goes to an excited state producing a 48-keV gamma ray. The specific activity of ^{238}U (0.332 nCi/mg) is small. This, coupled with the fact that gamma rays of this energy are highly absorbed, makes it difficult to detect ^{238}U as a pure source via gamma-ray spectroscopy. It can be detected, however, using the gamma rays from its first daughter (^{234}Th), provided that the two isotopes are in secular equilibrium. Secular equilibrium is defined as a condition such that the parent isotope and daughter are decaying with the same activity. This condition occurs (if the half life of the daughter is much less

(b) This work was done at the Oak Ridge Gaseous Diffusion Plant.
(c) Supplied by the Calutron Section of the Oak Ridge National Laboratory.

than that of the parent) after from seven to ten half lives of the daughter. Uranium-236, having a specific activity of 63.42 nCi/mg, was not present in the sources in sufficient quantity to be detected. It was treated here only for completeness.

Theoretical photon fluxes were calculated for the 238, 234, and 236 isotopes, using the decay schemes as given by Lederer, et al (1968). The ^{235}U calculation was made using the relative intensities given by Kroger (1972). A computer program was written to calculate this photon flux for each source, given the total weight of uranium on the source and the isotopic distribution in weight percent. This program is recorded in Figure 7. In calculating the theoretical gamma-ray flux, ^{234}Th (the first daughter of ^{238}U) was assumed to be in secular equilibrium with its parent isotope as the half life of the daughter is small compared to the parent. In the ^{235}U calculation, the following intensities were used: thorium K X rays (3.32%), 109 keV (2.5%), 143 keV (11%), 163 keV (5%), 183 keV (0.5%), 186 keV (54%), 195 keV (0.65%), 202 keV (0.8%), and 205 keV (5%). Lederer, et al (1968) list the K X-ray intensities of thorium as Kα2 (27%), Kα1 (48%), Kβ1 (18%), and Kβ2 (6%). Thus, the absolute intensities used in this calculation for the characteristic X rays were, respectively, 89.96 keV (0.90%), 93.35 keV (1.59%), 105 keV (0.6%), and 108.6 keV (0.2%). Decay schemes for each source are provided in Appendix B. Appendix C lists the sources used and the theoretical gamma-ray flux calculated for each.

RESULTS

Conclusions

During this work, gamma spectra were collected and calculated for various uranium sources of known isotopic distribution. The data were tabulated using existing computer programs which located and totaled each peak. Plots were also made, using existing computer programs. (These plots are given in Appendix D.) The gamma-ray peaks at 10.4, 237 and 249 keV are present in all the spectra collected, including the background run. Thus, they were reasonably attributed to background radiation. The low-energy gamma rays from ^{238}U (48 keV) and ^{236}U (49.8 keV) were easily converted to electrons and readily absorbed in the excitation of X rays. Those quanta which remained after these processes were not detected in the relatively short count times of this work. As a check, the collected and calculated data of this work were used to calculate an efficiency for the detector used. Since the efficiency of the detector was not known, it was tabulated via a computer program using the Newton-Coates method of numerical integration. As a rule, the experimentally derived efficiency was in agreement with the numerically integrated one. As can be seen by the results in Table 5, disagreement occurs at 53, 90, 109, 120.9, and 202 keV. Arguments and remarks that can be made relative to this disagreement follow.

The 53 and 120.9-keV peaks arise in the decay of ^{234}U. It is unknown why the efficiencies calculated for these peaks differ so greatly from the expected results. It is odd that the two results having the greatest difference should be common to the ^{234}U decay scheme. That they are common to the same decay scheme may imply inaccurate calculation of the ^{234}U decay data. There is also the implication that the source composition is not sufficiently well known, or that the decay and/or conversion data are not accurate enough to make the calculations. Should the source composition be inaccurate, the relative error should be the same for the 53.3-keV calculation as for the 120.9-keV calculation. That was not the case in

```
C-ORCAL6-8K-8/73

01.05 ERASE
01.06 T !!!!!!
01.10 A "       SOURCE NUMBER? "B
01.20 A "       MG TOTAL WEIGHT "C
01.30 A "       WEIGHT PERCENT 230-U "D;S D=D/100;S D=D/60
01.40 A "       WEIGHT PERCENT 236-U "I;S I=I/100;S I=I/60
01.50 A "       WEIGHT PERCENT 235-U "G;S G=G/100;S G=G/60
01.60 A "       WEIGHT PERCENT 234-U "H;S H=H/100;S H=H/60
01.70 S J=C*G*4762;S K=C*H*1.376E7;S L=C*D*737;S M=C*I*1.408E5;T !
01.80 T "       THEORETICAL GAMMA FLUX FOR SOURCE FOLLOWS: ",!!!!!!
01.90 T "        ISOTOPE            PHOTON ENERGY              PHOTONS",!

02.10 T "        DECAYING                KEV                    PER SEC",!
02.15 T "      "
02.20 T "  238-U                    48                 "L*0.1171,!!
02.35 D 2.15
02.30 T "  236-U                    49.8               "M*0.0006,!!
02.31 D 2.15
02.35 T "  234-U                    53.3               "K*0.0022,!!
02.36 D 2.15
02.40 T "  234-TH                   63                 "L*0.0211,!!
02.41 D 2.15
02.42 T "  KA2-TH                   89.96              "J*0.0090,!!
02.43 D 2.15
02.44 T "  234-TH                   93                 "L*0.0342,!!
02.45 D 2.15
02.46 T "  KA1-TH                   93.35              "J*0.0159,!!
02.47 D 2.15
02.48 T "  KB1-TH                  105.0               "J*0.0060,!!
02.49 D 2.15
02.50 T "  KB2-TH                  108.6               "J*0.0020,!!
02.51 D 2.15
02.52 T "  235-U                   109                 "J*0.0150,!!
02.55 D 2.15
02.60 T "  234-U                   120.9               "K*0.0035,!!
02.65 D 2.15
02.70 T "  235-U                   143                 "J*0.0970,!!
02.75 D 2.15
02.80 T "  238-U                   160                 "L*0.0023,!!
02.85 D 2.15
02.90 T "  235-U                   163                 "J*0.0460,!!
02.95 D 2.15

03.10 T "  235-U                   183                 "J*0.0046,!!
03.15 D 2.15
03.20 T "  235-U                   186                 "J*0.5400,!!
03.25 D 2.15
03.26 T "  235-U                   195                 "J*0.0065,!!
03.27 D 2.15
03.30 T "  235-U                   202                 "J*0.0105,!!
03.35 D 2.15
03.40 T "  235-U                   205                 "J*0.0490,!!
03.50 T !!!!!!
03.60 FOR X=1,1,11;DO ALL

04.10 QUIT
*
```

Figure 7. COMPUTER PROGRAM TO FIGURE DECAY IN PHOTONS PER SECOND WHEN GIVEN TOTAL WEIGHT OF URANIUM AND ISOTOPIC DISTRIBUTION IN WEIGHT PERCENT.

this work. Accordingly, new conversion ratios were calculated for these two photon energies.

The two error peaks at 90 and 109 keV fall in the characteristic X-ray region, thus suffering possible interference effects. In this region, with a calibration factor of 0.25 keV per channel, the peaks lie so close together that they could not be sufficiently resolved. Again,

Table 5

THE EXPERIMENTAL EFFICIENCY AND ABSORPTION-CORRECTED THEORETICAL EFFICIENCY FOUND IN THIS WORK

Photon Energy (keV)	Experimental Efficiency	Theoretical Efficiency
53	0.009	0.040
63	0.075	0.079
90	0.234	0.147
93	0.159	0.150
105	0.181	0.157
109	0.102	0.157
121	0.014	0.152
143	0.146	0.130
163	0.130	0.107
186	0.116	0.083
195	0.093	0.076
202	0.031	0.072
205	0.090	0.069

the possibility exists that the decay characteristics (in this case the abundance of the characteristic X rays) are not accurately known. For this reason, the abundances are calculated.

Errors at 202 keV can arise because the 202 and 205-keV photon peaks overlap in the multichannel analyzer. It is interesting to note that when the two experimental results are summed, the calculated efficiency (8.5%) more closely approximates the theoretical efficiency (7.0%). Again, on the possibility that the decay is not known to the required degree of accuracy, the abundance is calculated.

Thus, on the premise that inaccurate source data resulted in the error, the detector efficiency was used to try to calculate true decaying intensities. When the experimental efficiency agreed with the theoretical efficiency sufficiently well, it was used to calculate a relative intensity; otherwise, the theoretical value was utilized. The results of these calculations (found by dividing the ratio of the experimental to total activity of gamma and X-ray flux by the detector efficiency) are listed in Table 6. (The units of this calculated intensity are decays per 100 disintegrations of the uranium parent isotope under consideration.) As a result of this final calculation, the K characteristic X rays of thorium were found to represent 5.03% of the total ^{235}U activity. The ^{234}U activity present in Source 13M (the only source in which peaks representative of this isotope were found) was 514.434 nanocuries (nCi), or 1.90×10^4 disintegrations per second. The calculated intensities for the 53 and 120.9-keV photons were, respectively, 0.050 and 0.032. Comparing these values to those predicted by the alpha decay scheme, revealed conversion coefficients of 567 to 1 for the 53.3-keV photon and 10.94 to 1 for the 120.9-keV photon. The relative abundances for these two photons, along with those reported by Lederer, et al (1968), are reported in Table 7. Lederer, et al (1968) also list the conversion coefficient of the 53.3-keV photon as 130 to 1. However, from graphs in the appendixes of this source, the 53.3-keV photon conversion coefficient can be interpolated to be 357 to 1. Both the 53.3 and 120.9-keV transitions are E-2 transitions.

Other sources of error in this work were:

1. The theoretical efficiencies may have been biased high, particularly at the higher photon energies, if all those photons which undergo Compton scattering were not completely removed from the peak. This bias would result because only the photoelectric cross section was used in calculating the theoretical efficiency.

Table 6

PHOTON INTENSITY FROM URANIUM SOURCES IN UNITS OF PHOTONS PER 100 DISINTEGRATIONS OF THE PARENT URANIUM ISOTOPE

Photon Energy (keV)	Abundance in Photons per 100 Disintegrations	Abundance Given by Kroger (1972)	Parent Uranium Isotope
53.3	0.050	-	234
63	2.11	-	238
89.96	1.36	-	235
93	3.42	-	238
93.35	2.43	-	235
105.61	0.92	-	235
108.61	0.32	-	235
109	1.05	1.5	235
120.9	0.032	-	234
143	9.67	9.7	235
163	4.60	4.6	235
185.9	53.98	54.0	235
195	0.65	0.65	235
202	0.37	1.05	[illegible]
205	5.57	4.9	235

Table 7

RELATIVE ABUNDANCE OF ^{234}U GAMMA RAY PHOTONS

Photon Energy (keV)	Results of this Work	Results from Lederer, *et al*
53.3	100%	100%
120.9	64%	34%

2. Results for the source in the nylon sample vial were not corrected for absorption in the vial material or self absorption in the sample, and, thus, they may have been biased low.

Applications

It is anticipated that the results of this work could be applied to in vivo monitoring for the various isotopes of uranium. Monitoring of this nature already exists for the ^{235}U isotope. Such monitoring for ^{238}U utilizes the 93-keV gamma rays from the first daughter ^{234}Th in estimating lung burdens. Nearly all forms of uranium contain the ^{235}U isotope, which exhibits peaks in this region, thereby interfering with a ^{238}U determination. The peaks which provide this interference are the characteristic X rays of ^{231}Th, which are inherent in the decay of ^{235}U. Indeed, in some sources, the gamma activity becomes strong enough and intermixed enough such that the characteristic X rays of uranium were excited, which would also contribute to this interference. It has been demonstrated in this work that the 48-keV gamma ray from ^{238}U and the 49.8-keV gamma ray from ^{236}U could not be applied in in vivo monitoring. It is felt, however, that, given solid-state detection equipment and sufficiently long count times, the 53.3 and 120.9-keV photons could, at some future time, be considered feasible for use in in vivo monitoring for ^{234}U.

BIBLIOGRAPHY

Bearden, J. A.; "X-Ray Wavelengths", *Rev Mod Phys, 39*, p 78 (1967).

Cofield, R. E.; "In vivo Counting as a Measurement of Uranium in the Human Lung", *Health Physics, 2*, pp 269-287 (1960).

Crouthamel, C. E.; *Applied Gamma-Ray Spectrometry: Second Edition*, Revised and Enlarged by F. Adams and R. Dams; Pergamon Press, Oxford-New York-Toronto-Sydney-Braunschweig (1970).

Fine, S. and Hendee, C. F.; "X-Ray Critical Absorption and Emission Energies in keV", *Nucleonics, 13*, (3), p 36 (1965).

French, W. R., Jr, LaShure, R. L., and Curran, J. L.; "Lithium-Drifted Germanium Detectors", *Am J Phys, 37*, p 11 (1969).

Hyde, E. K., Perlman, I., and Seaborg, G. T.; *Nuclear Properties of the Heavy Elements, Vol II: Detailed Radioactivity Properties*; Prentice-Hall, Englewood Clifts, New Jersey (1964).

Kelly, M. T.; "ORCAL - A Conversational Calculating Language for the ND-812 Computer", *Oak Ridge National Laboratory Technical Manual*, ORNL-TM-3697 (1972).

Kroger, L. A.; *Level-Scheme Studies in 229-Th and 231-Th from the Alpha-Decay of 233-U and 235-U*, University of Wyoming, Ph. D. Thesis (1972).

Lederer, C. M., Hollander, J. M., and Perlman, I.; *Table of Isotopes*; John Wiley and Sons, New York (1968).

Martin, M. J. and Blichert-toft, P. H.; "Radioactive Atoms - Auger-Electrons, α-, β-, γ- and X-Ray Data, *Nuclear Data Tables, A8*, pp 1-198 (1970).

Palms, J. M., Venugopala Rao, P., and Wood, R. E.; "The Characteristics of an Ultra-High Resolution Ge(Li) Spectrometer for Singles and Coincidence X-Ray and Gamma Ray Studies", *IEEE Trans Nucl Sci*, NS-16, *1*, p 36 (1969).

Palms, J. M., Venugopala Rao, P., and Wood, R. E.; "An Ultra-High Resolution Ge(Li) Spectrometer for Singles and Coincidence X-Ray and Gamma Ray Studies", *Nucl Insts and Methods, 64*, p 310 (1968).

Stainer, H. M.; *X-Ray Mass Absorption Coefficients*, US Dept of the Interior: Bureau of Mines, IC-8166.

Stephens, F. S.; *Decay Schemes and Nuclear Spectroscopic States in the Heavy Element Region*, University of California Radiation Laboratory Report, UCRL 2970; June 1955.

Teoh, W., Conner, R. D., and Betts, R. H.; "The Decay of 235-U", *Nuclear Physics, A228 (3)*, p 432 (1974).

Van Hull, A. K.; ***Personal Conversation***; Union Carbide Corporation-Nuclear Division, Oak Ridge Y-12 Plant, Oak Ridge, Tennessee.

Vegors, S. H., Jr, Marsden, L. L., and Heath, R. L.; ***Calculated Efficiencies of Cylindrical Radiation Detectors***, AEC Research and Development Report IDO-16370; September 1958.

Victoreen, J. A.; "The Calculation of X-Ray Mass Absorption Coefficients", ***J Appl Phys, 11*** pp 1141-1147 (1949).

Vorob'ev, A. A., Komar, A. P., and Korolev, V. A.; "Investigation of Alpha Decay of 235-U by Means of an Ionization, Alpha-Spectrometer", ***Bull Aca Sci USSR***, Phys Ser 24, p 1099 (1960).

APPENDIX A

COMPUTER PROGRAM TO FIGURE THEORETICAL EFFICIENCY

```
LEVEL  21.6  (DEC 72)                    OS/360  FORTRAN H                    DATE  75.245/20.25.50

          COMPILER OPTIONS - NAME=  MAIN,OPT=02,LINECNT=60,SIZE=0000K,
                             SOURCE,EBCDIC,NOLIST,NODECK,LOAD,MAP,NOEDIT,ID,XREF
   ISN 0002           IMPLICIT REAL*8 (A-H,O-Z)
   ISN 0003           EXTERNAL FFUN,SFUN
   ISN 0004           DIMENSION A(100),B(100),X(100),Y(100),C(100),D(100)
   ISN 0005           COMMON /TS/ R,TAU,H,BS,T
   ISN 0006           COMMON /ARG/ XI,XJ
   ISN 0007           PI = DARCOS(-1.0D0)
   ISN 0008         1 CONTINUE
   ISN 0009           READ(5,5000) R,BS,T,H,E,TAU,NSEG
   ISN 0010      5000 FORMAT(6F10.0,I10)
   ISN 0011           IF ( NSEG .GT. 100) NSEG = 97
   ISN 0013           IF(NSEG .LE. 0 ) NSEG = 22
   ISN 0015           GO TO 2
   ISN 0016         3 NSEG = NSEG + 1
   ISN 0017         2 IF ( MOD(NSEG,4) .NE. 1 ) GO TO 3
   ISN 0019           WRITE(6,6001) E,R,BS,T,H,TAU,NSEG
   ISN 0020      6001 FORMAT( '1',10X,' EVALUATION OF DETECTOR EFFICIENCY FOR ',F5.1,' K
                     1EV'/
                     1'0',10X,'DISK RADIUS              ',F10.5/
                     1'0',10X,'DETECTOR RADIUS          ',F10.5/
                     1'0',10X,'DETECTOR HEIGHT          ',F10.5/
                     1'0',10X,'DETECTOR TO SOURCE DISP ',F10.5/
                     1'0',10X,'LINEAR ABSORPTION COEFFICIENT',F10.5/
                     1'0',10X,'SEGMENTS FOR INTEGRATION',I10)
   ISN 0021           DELI = R/(NSEG-1)
   ISN 0022           DELJ = PI/(NSEG-1)
   ISN 0023           BI = 0.0
   ISN 0024           DO 200 I = 1,NSEG
   ISN 0025           XI = BI + (I-1)*DELI
   ISN 0026           BJ = -PI/2.0
   ISN 0027           DO 100 J = 1,NSEG
   ISN 0028           XJ = BJ+ (J-1)*DELJ
   ISN 0029           DUM = -XI*DSIN(XJ)+DSQRT(XI**2*DSIN(XJ)**2-(XI**2-RS**2))
   ISN 0030           FU = DATAN(DUM/(H+T))
   ISN 0031           FL = 0.0
   ISN 0032           SU = DATAN(DUM/H)
   ISN 0033           SL = FU
   ISN 0034           DELK = (FU-FL)/(NSEG-1)
   ISN 0035           DELM = (SU-SL)/(NSEG-1)
   ISN 0036           XINC=0
   ISN 0037           DO 75 KK=1,NSEG
   ISN 0038           C(KK)=FFUN(XINC)
   ISN 0039           XINC=XINC+DELK
   ISN 0040        75 CONTINUE
   ISN 0041           XINC=FU
   ISN 0042           DO 85 KK=1,NSEG
   ISN 0043           D(KK)=SFUN(XINC)
   ISN 0044           XINC=XINC+DELM
   ISN 0045        85 CONTINUE
   ISN 0046           CALL NEWCT5(C,DELK,NSEG,SDUM2)
   ISN 0047           CALL NEWCT5(D,DELM,NSEG,SDUM3)
   ISN 0048           X(J) = SDUM2 + SDUM3
   ISN 0049       100 CONTINUE
   ISN 0050           CALL NEWCT5(X,DELJ,NSEG,SDUM1)
   ISN 0051           Y(I) = SDUM1*XI
   ISN 0052       200 CONTINUE
   ISN 0053           CALL NEWCT5(Y,DELI,NSEG,SDUM1)

   ISN 0054           XINTR = SDUM1/(PI*R*R)
   ISN 0055           WRITE(6,6000) XINTR
   ISN 0056      6000 FORMAT('0',10X,'EFFICIENCY (INTEGRAL)    ',D16.8)
   ISN 0057           GO TO 1
   ISN 0058           STOP
   ISN 0059           END

LEVEL  21.6  (DEC 72)                    OS/360  FORTRAN H                    DATE  75.245/20.25.54

          COMPILER OPTIONS - NAME=  MAIN,OPT=02,LINECNT=60,SIZE=0000K,
                             SOURCE,EBCDIC,NOLIST,NODECK,LOAD,MAP,NOEDIT,ID,XREF
   ISN 0002           DOUBLE PRECISION FUNCTION FFUN(X)
   ISN 0003           IMPLICIT REAL*8 (A-H,O-Z)
   ISN 0004           COMMON /TS/ R,TAU,H,BS,T
   ISN 0005           T1 = DEXP(-TAU*T/DCOS(X))
   ISN 0006           FFUN = (1.0-T1)*DSIN(X)
   ISN 0007           RETURN
   ISN 0008           END
```

```
LEVEL  21.6  (DEC 72)                          OS/360  FORTRAN H                          DATE  75.243/20.25.57

          COMPILER OPTIONS - NAME=  MAIN,OPT=02,LINECNT=60,SIZE=0000K,
                             SOURCE,EBCDIC,NOLIST,NODECK,LOAD,MAP,NOEDIT,ID,XREF
   ISN 0002           DOUBLE PRECISION FUNCTION SFUN(X)
   ISN 0003           IMPLICIT REAL*8 (A-H,O-Z)
   ISN 0004           COMMON /TS/ B,TAU,H,BS,T
   ISN 0005           COMMON /ARG/ XI,XJ
   ISN 0006           T1 =(-XI*DSIN(XJ)+DSQRT(XI*XI*DSIN(XJ)**2-(XI**2-BS**2)))/DSIN(X )
                     1 -H/DCOS(X )
   ISN 0007           T2 = DEXP(-TAU*T1)
   ISN 0008           SFUN = (1.   T2           )*DSIN(X )
   ISN 0009           RETURN
   ISN 0010           END


LEVEL  21.6  (DEC 72)                          OS/360  FORTRAN H                          DATE  75.243/20.26.01

          COMPILER OPTIONS - NAME=  MAIN,OPT=02,LINECNT=60,SIZE=0000K,
                             SOURCE,EBCDIC,NOLIST,NODECK,LOAD,MAP,NOEDIT,ID,XREF
   ISN 0002           SUBROUTINE NEWCTS(X,DEL,N,XINT)
   ISN 0003           IMPLICIT REAL*8 (A-H,O-Z)
   ISN 0004           DIMENSION X(1)
   ISN 0005           SUM = 0.0
   ISN 0006           FACT = 2.0*DEL/45.
   ISN 0007           N1 = N - 1
   ISN 0008           DO 10 I = 2,N1,2
   ISN 0009           SUM = SUM + 32.0 * FACT * X(I)
   ISN 0010        10 CONTINUE
   ISN 0011           N2 = N-2
   ISN 0012           DO 20 I = 3,N2,4
   ISN 0013           SUM = SUM + 12.0 * FACT * X(I)
   ISN 0014        20 CONTINUE
   ISN 0015           N4 = N - 4
   ISN 0016           DO 30 I = 5,N4,4
   ISN 0017           SUM = SUM + 14.0 * FACT * X(I)
   ISN 0018        30 CONTINUE
   ISN 0019           SUM = SUM + 7.0 * FACT *(X(1)+X(N))
   ISN 0020           XINT = SUM
   ISN 0021           RETURN
   ISN 0022           END
```

```
 EVALUATION OF DETECTOR EFFICIENCY FOR  53.0 KEV

DISK RADIUS                1.90500

DETECTOR RADIUS            2.15000

DETECTOR HEIGHT            1.60000

DETECTOR TO SOURCE DISP    0.77000

LINEAR ABSORPTION COEFFICIENT  13.01300

SEGMENTS FOR INTEGRATION       53

EFFICIENCY (INTEGRAL)     0.270327970 00
```

```
 EVALUATION OF DETECTOR EFFICIENCY FOR  63.0 KEV

DISK RADIUS                1.90500

DETECTOR RADIUS            2.15000

DETECTOR HEIGHT            1.60000

DETECTOR TO SOURCE DISP    0.77000

LINEAR ABSORPTION COEFFICIENT   7.98740

SEGMENTS FOR INTEGRATION       53

EFFICIENCY (INTEGRAL)     0.266151170 00
```

EVALUATION OF DETECTOR EFFICIENCY FOR 90.0 KEV

DISK RADIUS	1.90500
DETECTOR RADIUS	2.15000
DETECTOR HEIGHT	1.60000
DETECTOR TO SOURCE DISP	0.77000
LINEAR ABSORPTION COEFFICIENT	2.81360
SEGMENTS FOR INTEGRATION	53
EFFICIENCY (INTEGRAL)	0.24641909D 00

EVALUATION OF DETECTOR EFFICIENCY FOR 93.0 KEV

DISK RADIUS	1.90500
DETECTOR RADIUS	2.15000
DETECTOR HEIGHT	1.60000
DETECTOR TO SOURCE DISP	0.77000
LINEAR ABSORPTION COEFFICIENT	2.55210
SEGMENTS FOR INTEGRATION	53
EFFICIENCY (INTEGRAL)	0.24320026D 00

EVALUATION OF DETECTOR EFFICIENCY FOR 105.0 KEV

DISK RADIUS	1.90500
DETECTOR RADIUS	2.15000
DETECTOR HEIGHT	1.60000
DETECTOR TO SOURCE DISP	0.77000
LINEAR ABSORPTION COEFFICIENT	1.78640
SEGMENTS FOR INTEGRATION	53
EFFICIENCY (INTEGRAL)	0.23794542D 00

EVALUATION OF DETECTOR EFFICIENCY FOR 109.0 KEV

DISK RADIUS	1.90500
DETECTOR RADIUS	2.15000
DETECTOR HEIGHT	1.60000
DETECTOR TO SOURCE DISP	0.77000
LINEAR ABSORPTION COEFFICIENT	1.60040
SEGMENTS FOR INTEGRATION	53
EFFICIENCY (INTEGRAL)	0.22198602D 00

EVALUATION OF DETECTOR EFFICIENCY FOR 121.0 KEV

DISK RADIUS	1.90500
DETECTOR RADIUS	2.15000
DETECTOR HEIGHT	1.60000
DETECTOR TO SOURCE DISP	0.77000
LINEAR ABSORPTION COEFFICIENT	1.17670
SEGMENTS FOR INTEGRATION	53
EFFICIENCY (INTEGRAL)	0.20206657D 00

EVALUATION OF DETECTOR EFFICIENCY FOR 143.0 KEV

DISK RADIUS	1.90500
DETECTOR RADIUS	2.15000
DETECTOR HEIGHT	1.60000
DETECTOR TO SOURCE DISP	0.77000
LINEAR ABSORPTION COEFFICIENT	0.71890
SEGMENTS FOR INTEGRATION	53
EFFICIENCY (INTEGRAL)	0.16251586D 00

EVALUATION OF DETECTOR EFFICIENCY FOR 163.0 KEV

DISK RADIUS	1.90500
DETECTOR RADIUS	2.15000
DETECTOR HEIGHT	1.60000
DETECTOR TO SOURCE DISP	0.77000
LINEAR ABSORPTION COEFFICIENT	0.48831
SEGMENTS FOR INTEGRATION	53
EFFICIENCY (INTEGRAL)	0.12945726D 00

EVALUATION OF DETECTOR EFFICIENCY FOR 196.0 KEV

DISK RADIUS	1.90500
DETECTOR RADIUS	2.15000
DETECTOR HEIGHT	1.60000
DETECTOR TO SOURCE DISP	0.77000
LINEAR ABSORPTION COEFFICIENT	0.33039
SEGMENTS FOR INTEGRATION	53
EFFICIENCY (INTEGRAL)	0.98587881D-01

EVALUATION OF DETECTOR EFFICIENCY FOR 195.0 KEV

DISK RADIUS	1.90500
DETECTOR RADIUS	2.15000
DETECTOR HEIGHT	1.60000
DETECTOR TO SOURCE DISP	0.77000
LINEAR ABSORPTION COEFFICIENT	0.28723
SEGMENTS FOR INTEGRATION	53
EFFICIENCY (INTEGRAL)	0.88646268D-01

EVALUATION OF DETECTOR EFFICIENCY FOR 202.0 KEV

DISK RADIUS	1.90500
DETECTOR RADIUS	2.15000
DETECTOR HEIGHT	1.60000
DETECTOR TO SOURCE DISP	0.77000
LINEAR ABSORPTION COEFFICIENT	0.26255
SEGMENTS FOR INTEGRATION	53
EFFICIENCY (INTEGRAL)	0.82628342D-01

EVALUATION OF DETECTOR EFFICIENCY FOR 205.0 KEV

DISK RADIUS	1.90500
DETECTOR RADIUS	2.15000
DETECTOR HEIGHT	1.60000
DETECTOR TO SOURCE DISP	0.77000
LINEAR ABSORPTION COEFFICIENT	0.25126
SEGMENTS FOR INTEGRATION	53
EFFICIENCY (INTEGRAL)	0.79790551D-01

APPENDIX B

DECAY SCHEMES

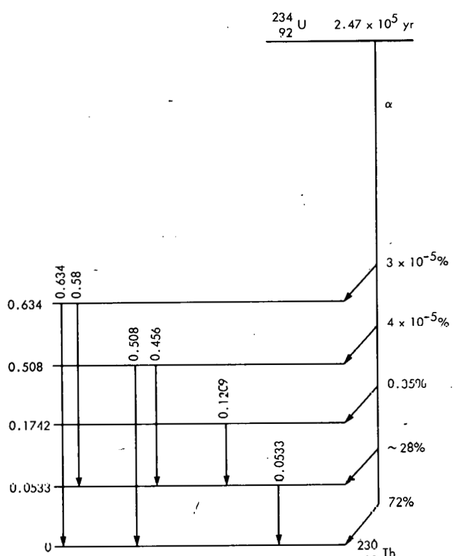

Figure B-1. URANIUM 234 DECAY SCHEME.

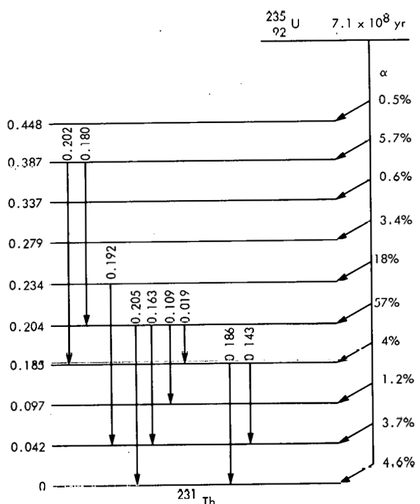

Figure B-2. URANIUM 235 DECAY SCHEME.

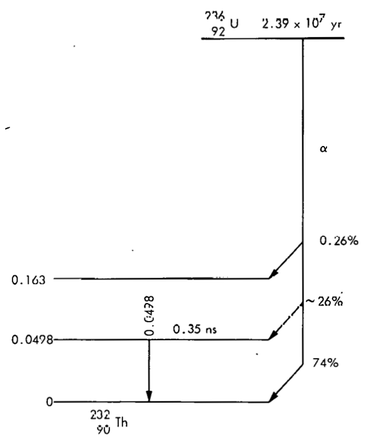

Figure B-3. URANIUM 236 DECAY SCHEME.

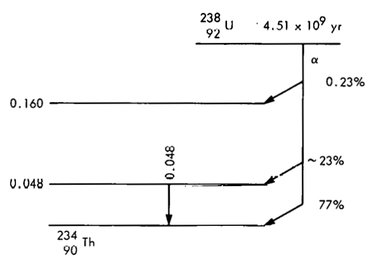

Figure B-4. URANIUM 238 DECAY SCHEME.

APPENDIX C

THEORETICAL GAMMA YIELD CALCULATIONS MADE USING KROGER (1972) DATA

Table C-1

THEORETICAL GAMMA FLUX OF SOURCE 8M

SOURCE NUMBER? :8M
MG TOTAL WEIGHT :8.0
WEIGHT PERCENT 238-U :97.959
WEIGHT PERCENT 236-U :0.0164
WEIGHT PERCENT 235-U :2.013
WEIGHT PERCENT 234-U :0.0123

THEORETICAL GAMMA FLUX FOR SOURCE FOLLOWS:

ISOTOPE DECAYING	PHOTON ENERGY KEV	PHOTONS PER SEC
238-U	48	11.2722
236-U	49.8	0.0080
234-U	53.3	0.4965
234-TH	63	2.0311
KA2-TH	89.96	0.1150
234-TH	93	3.0981
KA1-TH	93.35	0.2032
KB1-TH	105.0	0.0767
KB2-TH	108.6	0.0256
235-U	109	0.1917
234-U	120.9	0.7898
235-U	143	1.2398
238-U	160	0.2214
235-U	163	3.5879
235-U	183	0.0588
235-U	186	6.9019
235-U	195	0.0831
235-U	202	0.1342
235-U	205	0.6263

Table C-2

THEORETICAL GAMMA FLUX OF SOURCE 9M

SOURCE NUMBER? :9M
MG TOTAL WEIGHT :8.0
WEIGHT PERCENT 238-U :96.953
WEIGHT PERCENT 236-U :0.0202
WEIGHT PERCENT 235-U :3.009
WEIGHT PERCENT 234-U :0.0187

THEORETICAL GAMMA FLUX FOR SOURCE FOLLOWS:

ISOTOPE DECAYING	PHOTON ENERGY KEV	PHOTONS PER SEC
238-U	48	11.1564
236-U	49.8	0.0099
234-U	53.3	0.7548
234-TH	63	2.0103
KA2 TH	89.96	0.1720
234 TH	93	3.2583
KA1-TH	93.35	0.3038
KB1-TH	105.0	0.1146
KB2-TH	108.6	0.0382
235-U	109	0.2866
234-U	120.9	1.2008
235-U	143	1.8532
238-U	160	0.2191
235-U	163	0.8788
235-U	183	0.0879
235-U	186	10.3168
235-U	195	0.1242
235-U	202	0.2006
235-U	205	0.9362

Table C-3

THEORETICAL GAMMA FLUX OF SOURCE 10M

SOURCE NUMBER? :10M
MG TOTAL WEIGHT :8.0
WEIGHT PERCENT 238-U :94.6639
WEIGHT PERCENT 236-U :0.0438
WEIGHT PERCENT 235-U :5.2641
WEIGHT PERCENT 234-U :0.0282

THEORETICAL GAMMA FLUX FOR SOURCE FOLLOWS:

ISOTOPE DECAYING	PHOTON ENERGY KEV	PHOTONS PER SEC
238-U	48	10.8930
236-U	49.8	0.0214
234-U	53.3	1.1382
234-TH	63	1.9628
KA2 TH	89.96	0.3008
234-TH	93	3.1814
KA1-TH	93.35	0.5314
KB1-TH	105.0	0.2006
KB2-TH	108.6	0.0669
235-U	109	0.5014
234-U	120.9	1.8108
235-U	143	3.2421
238-U	160	0.2140
235-U	163	1.5375
235-U	183	0.1538
235-U	186	18.0487
235-U	195	0.2173
235-U	202	0.3510
235-U	205	1.6378

Table C-4

THEORETICAL GAMMA FLUX OF SOURCE 11M

SOURCE NUMBER? :11M
MG TOTAL WEIGHT :8.0
WEIGHT PERCENT 238-U :93.6797
WEIGHT PERCENT 236-U :0.0306
WEIGHT PERCENT 235-U :6.2485
WEIGHT PERCENT 234-U :0.0412

THEORETICAL GAMMA FLUX FOR SOURCE FOLLOWS:

ISOTOPE DECAYING	PHOTON ENERGY KEV	PHOTONS PER SEC
238-U	48	10.7798
236-U	49.8	0.0149
234-U	53.3	1.6630
234-TH	63	1.9424
KA2-TH	89.96	0.3571
234-TH	93	3.1483
KA1-TH	93.35	0.6308
KB1-TH	105.0	0.2381
KB2-TH	108.6	0.0794
235-U	109	0.5951
234-U	120.9	2.6456
235-U	143	3.8484
238-U	160	0.2117
235-U	163	1.8250
235-U	183	0.1825
235-U	186	21.4239
235-U	195	0.2579
235-U	202	0.4166
235-U	205	1.9440

Table C-5

THEORETICAL GAMMA FLUX OF SOURCE 12M

SOURCE NUMBER? :12M
MG TOTAL WEIGHT :8.0
WEIGHT PERCENT 238-U :91.9373
WEIGHT PERCENT 236-U :0.0349
WEIGHT PERCENT 235-U :7.9748
WEIGHT PERCENT 234-U :0.0530

THEORETICAL GAMMA FLUX FOR SOURCE FOLLOWS:

ISOTOPE DECAYING	PHOTON ENERGY KEV	PHOTONS PER SEC
238-U	48	10.5793
236-U	49.8	0.0170
234-U	53.3	2.1392
234-TH	63	1.9063
KA2-TH	89.96	0.4557
234-TH	93.	3.0898
KA1-TH	93.35	0.8051
KB1-TH	105.0	0.3038
KB2-TH	108.6	0.1013
235-U	109	0.7595
234-U	120.9	3.4033
235-U	143	4.9116
238-U	160	0.2078
235-U	163	2.3292
235-U	183	0.2329
235-U	186	27.3427
235-U	195	0.3291
235-U	202	0.5317
235-U	205	2.4811

Table C-6

THEORETICAL GAMMA FLUX OF SOURCE 13M

SOURCE NUMBER? :13M
MG TOTAL WEIGHT :4.994
WEIGHT PERCENT 238-U :0.5296
WEIGHT PERCENT 236-U :0.1497
WEIGHT PERCENT 235-U :97.6630
WEIGHT PERCENT 234-U :1.6582

THEORETICAL GAMMA FLUX FOR SOURCE FOLLOWS:

ISOTOPE DECAYING	PHOTON ENERGY KEV	PHOTONS PER SEC
238-U	48	0.0381
236-U	49.8	0.0456
234-U	53.3	41.7807
234-TH	63	0.0069
KA2-TH	89.96	3.4839
234-TH	93	0.0111
KA1-TH	93.35	6.1548
KB1-TH	105.0	2.3226
KB2-TH	108.6	0.7742
235-U	109	5.8064
234-U	120.9	66.4698
235-U	143	37.5481
238-U	160	0.0008
235-U	163	17.8063
235-U	183	1.7806
235-U	186	209.0310
235-U	195	2.5161
235-U	202	4.0645
235-U	205	18.9676

Table C-7

THEORETICAL GAMMA FLUX OF SOURCE 14M

SOURCE NUMBER? :14M
MG TOTAL WEIGHT :10.1
WEIGHT PERCENT 238-U :0.06
WEIGHT PERCENT 236-U :0.038
WEIGHT PERCENT 235-U :99.834
WEIGHT PERCENT 234-U :0.06

THEORETICAL GAMMA FLUX FOR SOURCE FOLLOWS:

ISOTOPE DECAYING	PHOTON ENERGY KEV	PHOTONS PER SEC
238-U	48	0.0087
236-U	49.8	0.0234
234-U	53.3	3.0575
234-TH	63	0.0016
KA2-TH	89.96	7.2025
234-TH	93	0.0026
KA1-TH	93.35	12.7243
KB1-TH	105.0	4.8016
KB2-TH	108.6	1.6006
235-U	109	12.0041
234-U	120.9	4.8649
235-U	143	77.6264
238-U	160	0.0002
235-U	163	36.8125
235-U	183	3.6813
235-U	186	432.1470
235-U	195	5.2018
235-U	202	8.4029
235-U	205	39.2133

Table C-8

THEORETICAL GAMMA FLUX OF SOURCE 15M

SOURCE NUMBER? :15M
MG TOTAL WEIGHT :10.3
WEIGHT PERCENT 238-U :99.7635
WEIGHT PERCENT 236-U :0.01
WEIGHT PERCENT 235-U :0.3731
WEIGHT PERCENT 234-U :0.0096

THEORETICAL GAMMA FLUX FOR SOURCE FOLLOWS:

ISOTOPE DECAYING	PHOTON ENERGY KEV	PHOTONS PER SEC
238-U	48	14.7803
236-U	49.8	0.0063
234-U	53.3	0.4989
234-TH	63	2.6632
KA2-TH	89.96	0.0275
234-TH	93	4.3167
KA1-TH	93.35	0.0485
KB1-TH	105.0	0.0183
KB2-TH	108.6	0.0061
235-U	109	0.0458
234-U	120.9	0.7937
235-U	143	0.2959
238-U	160	0.2903
235-U	163	0.1403
235-U	183	0.0140
235-U	186	1.6470
235-U	195	0.0198
235-U	202	0.0320
235-U	205	0.1495

APPENDIX D

GAMMA SPECTRA

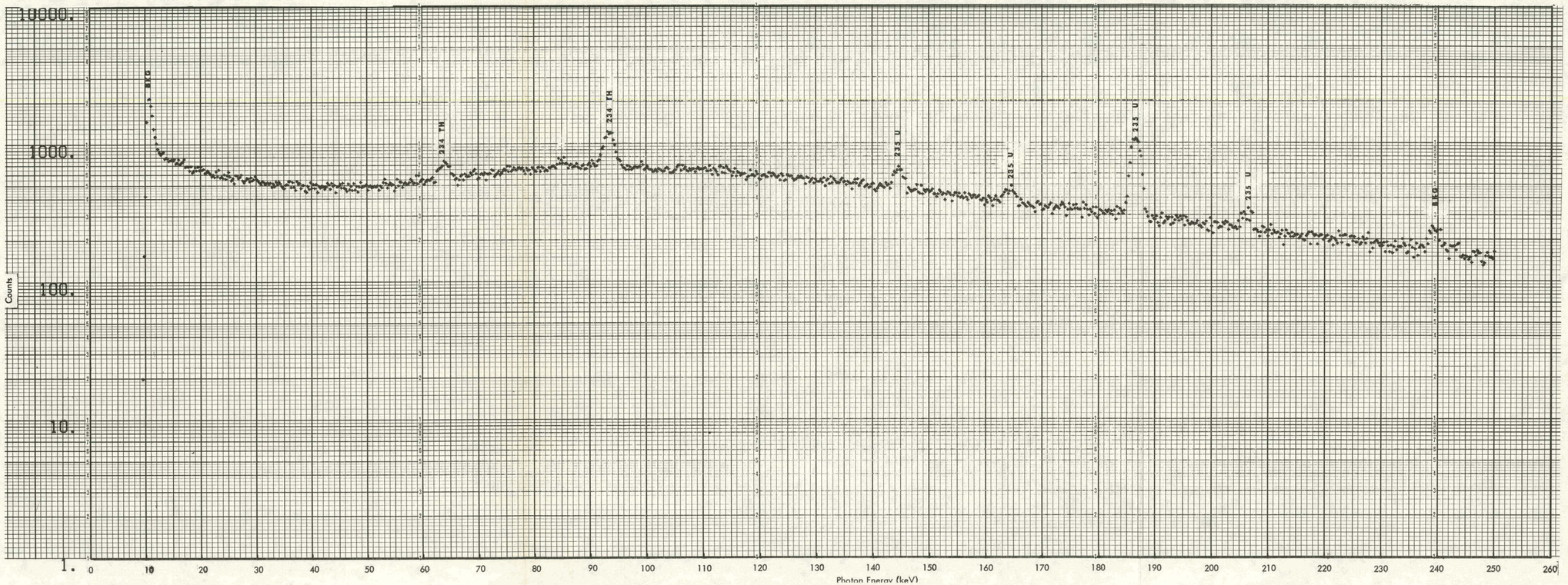

Figure D-1. GAMMA SPECTRUM OF SOURCE 8M.

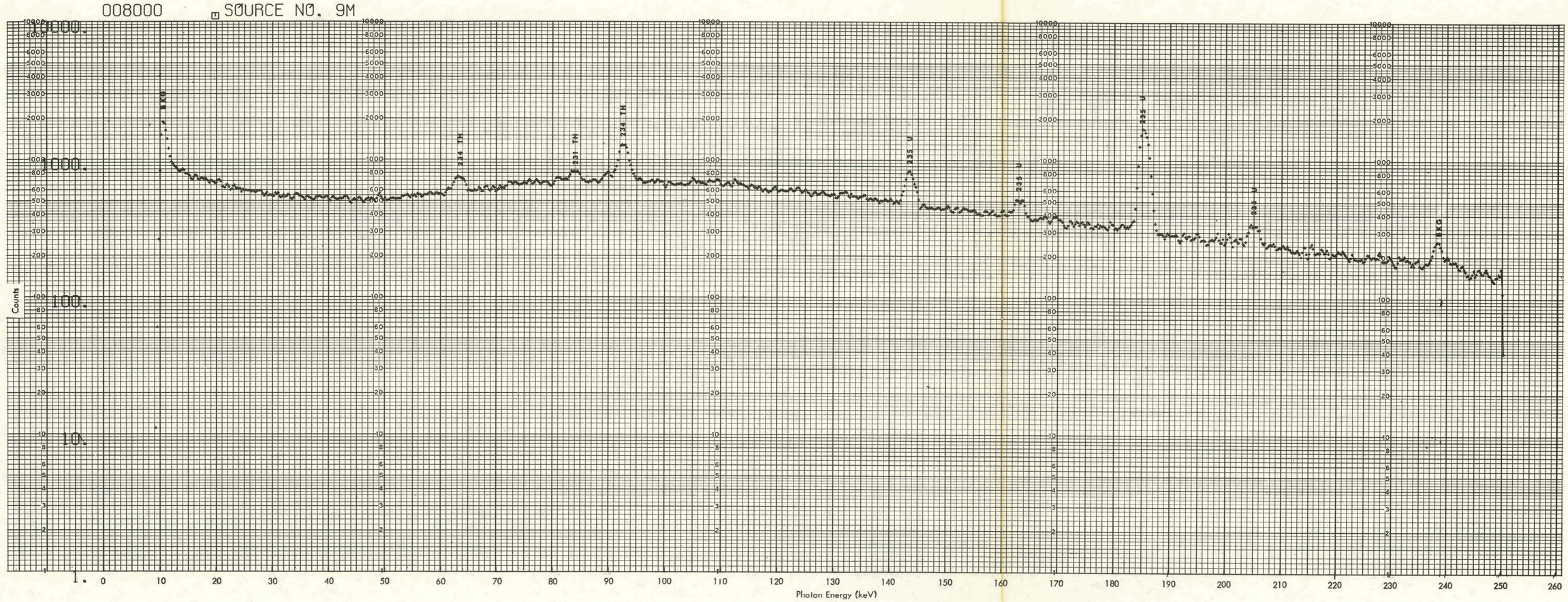

Figure D-2. GAMMA SPECTRUM OF SOURCE 9M.

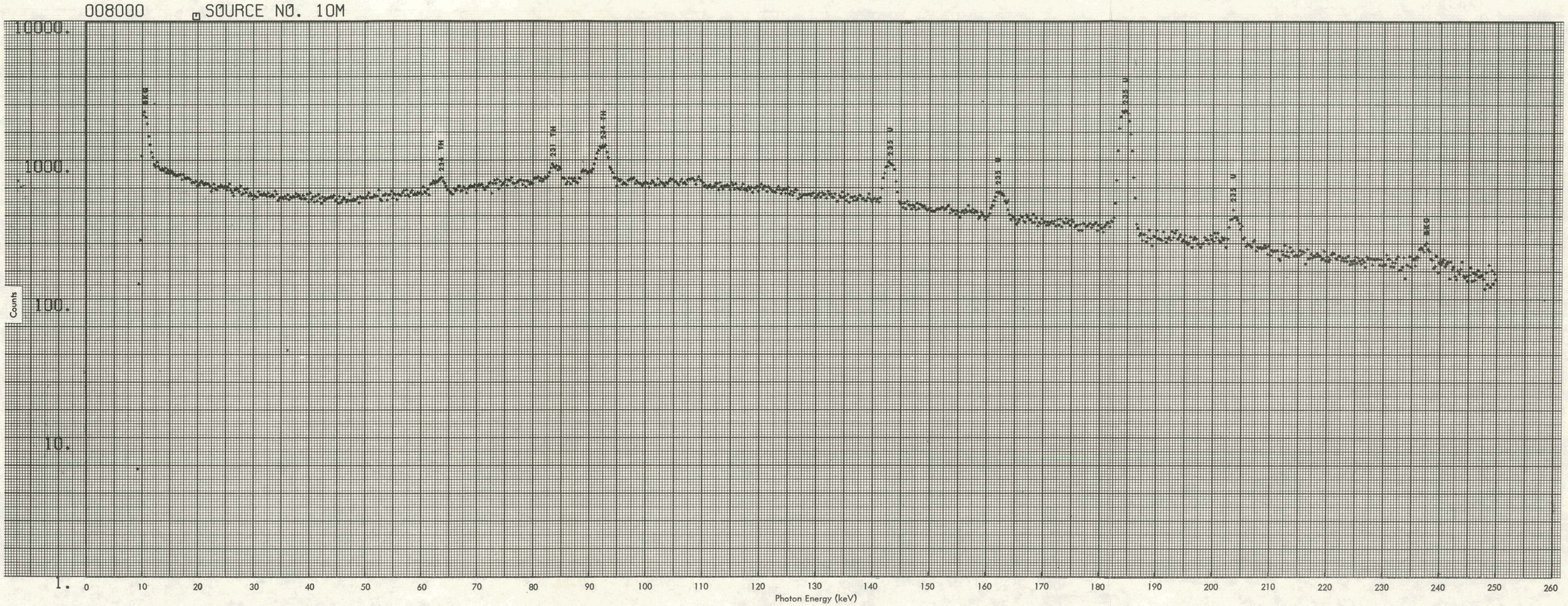

Figure D-3. GAMMA SPECTRUM OF SOURCE 10M.

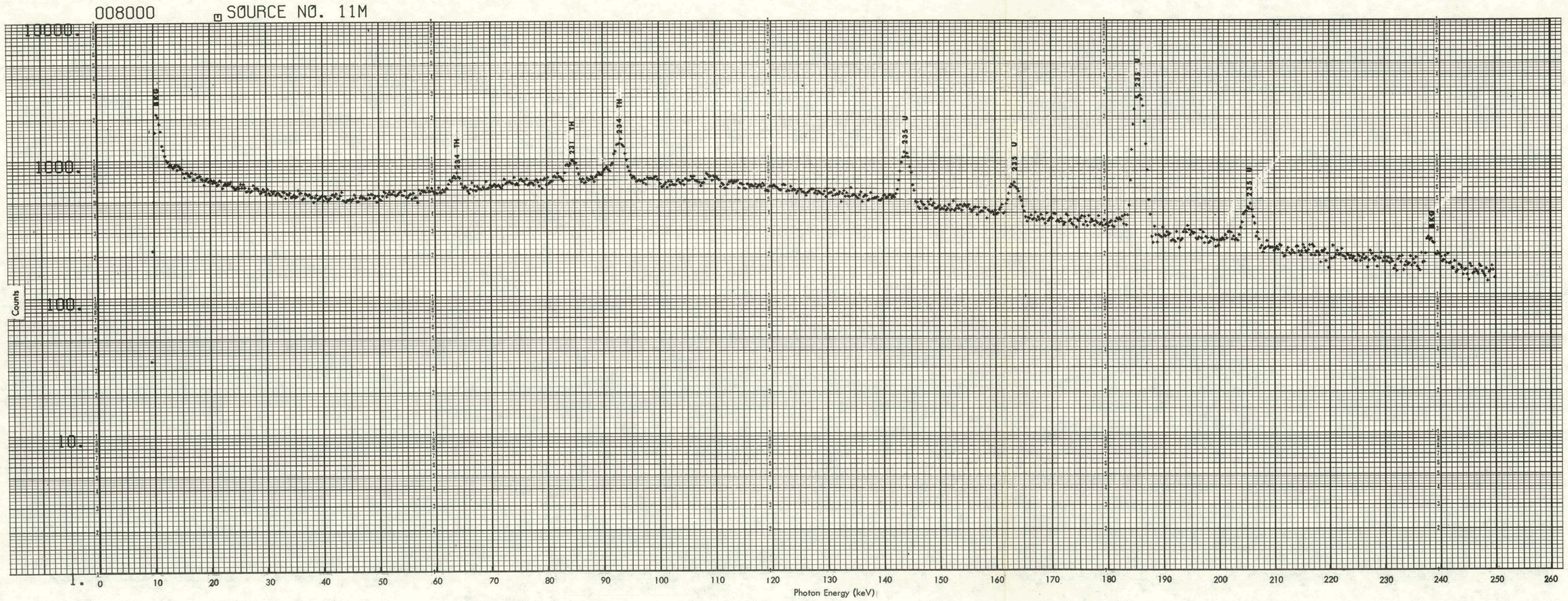

Figure D-4. GAMMA SPECTRUM OF SOURCE 11M.

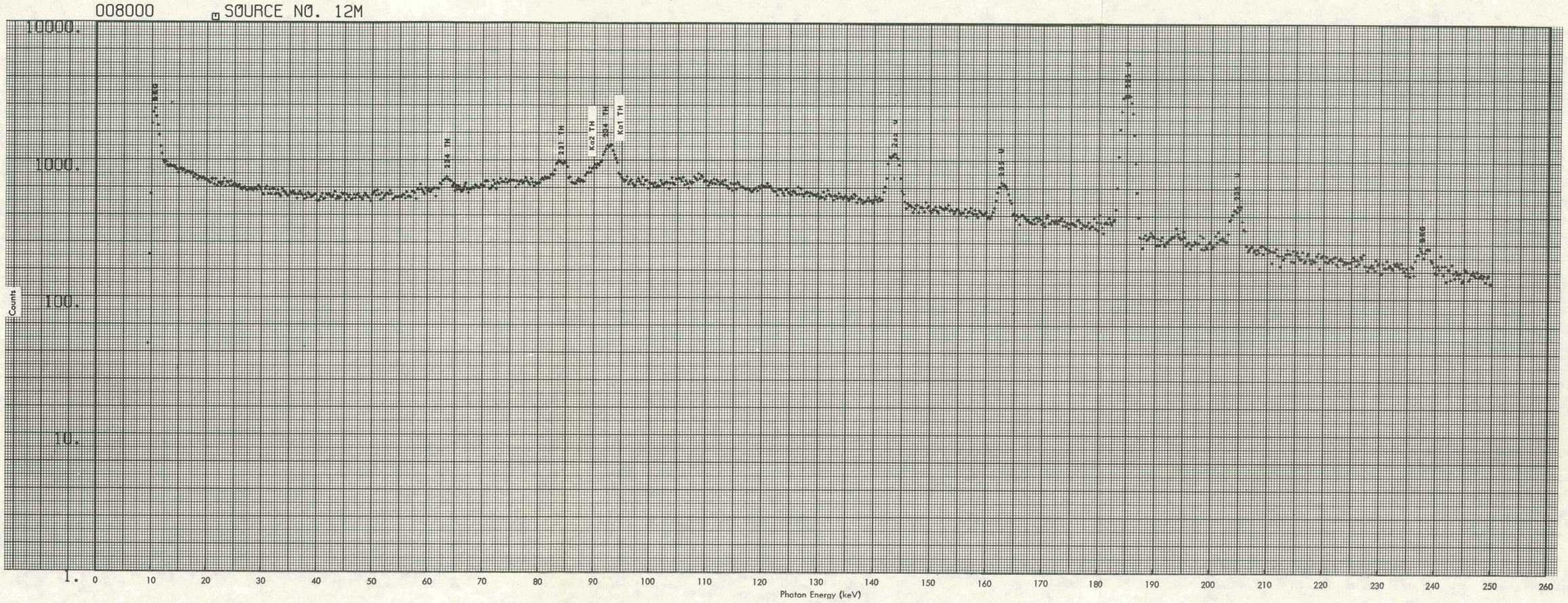

Figure D-5. GAMMA SPECTRUM OF SOURCE NUMBER 12M.

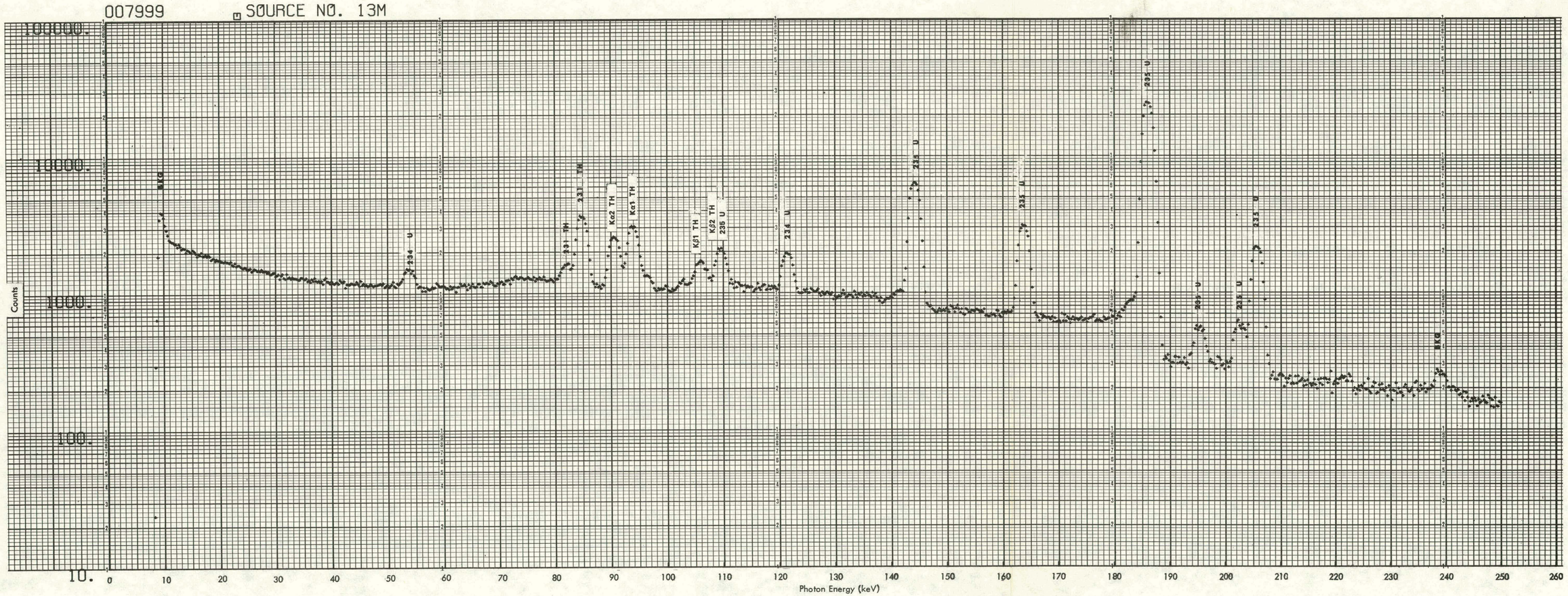

Figure D-6. GAMMA SPECTRUM OF SOURCE 13M.

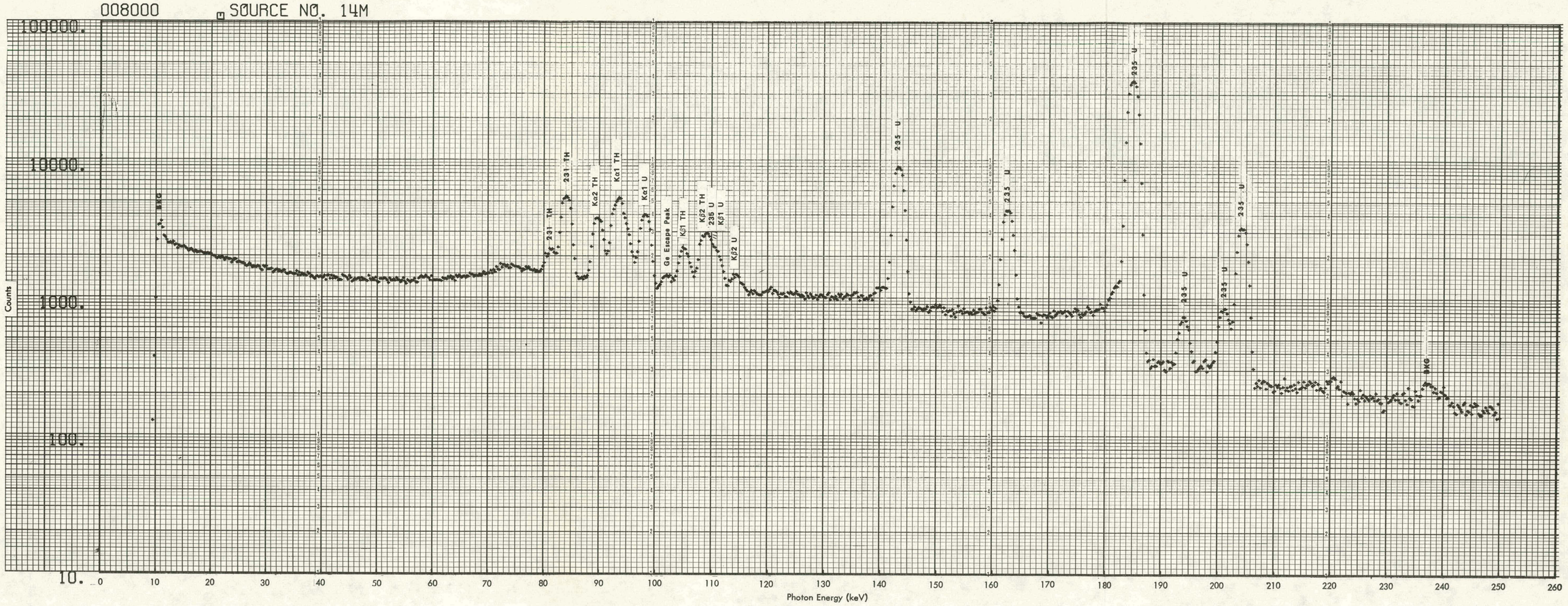

Figure D-7. GAMMA SPECTRUM OF SOURCE 14M.

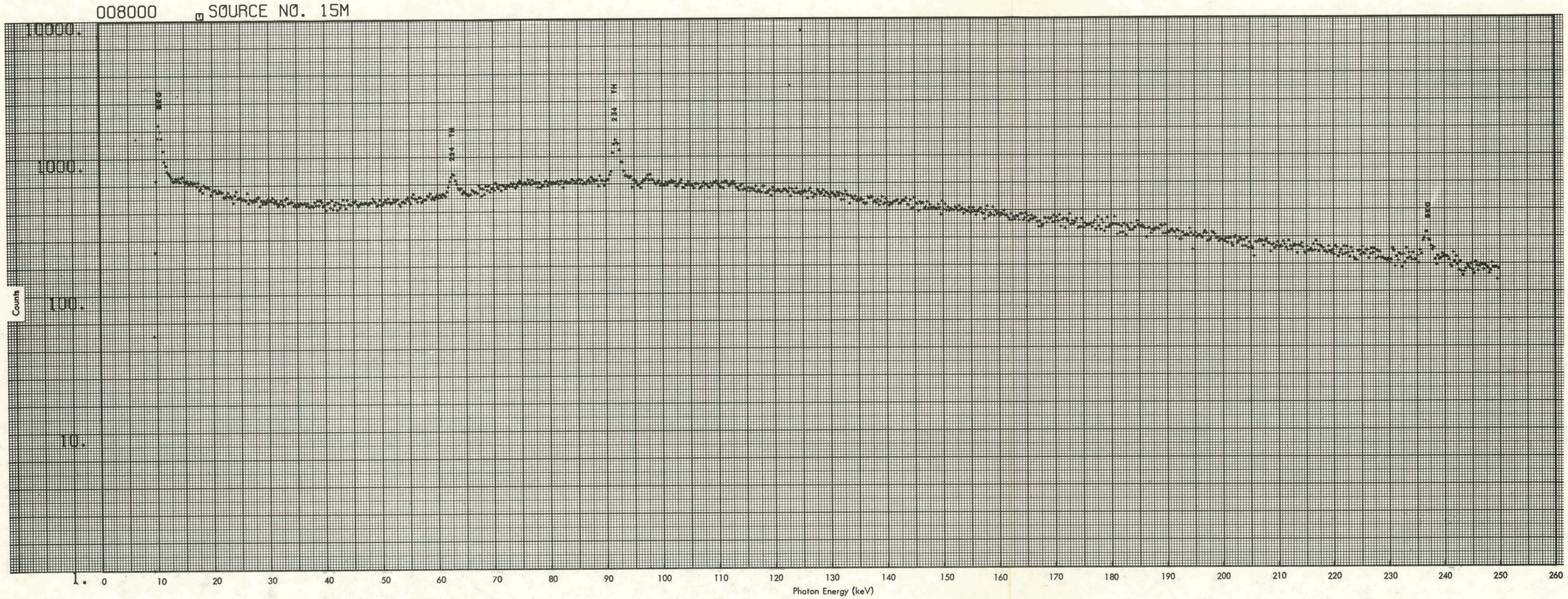

Figure D-8. GAMMA SPECTRUM OF SOURCE 15M.

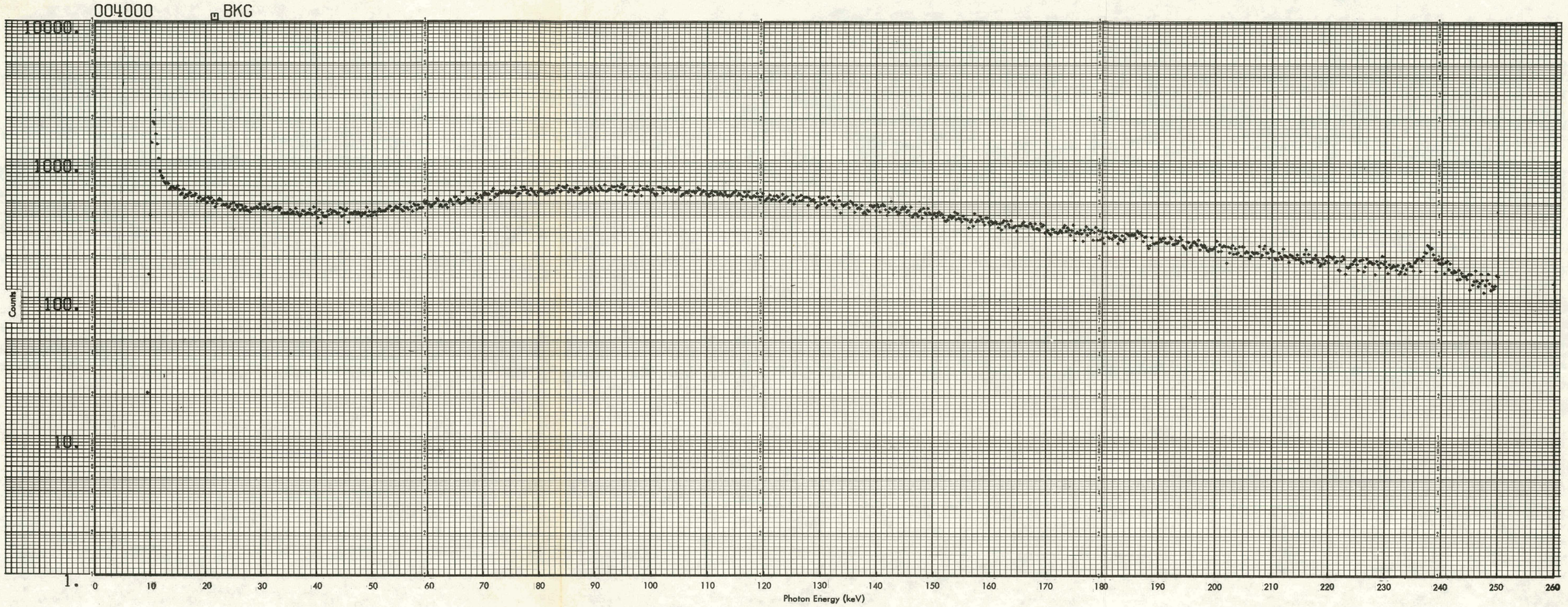

Figure D-9. BACKGROUND GAMMA SPECTRUM.

Distribution

Energy Research and Development Administration - Oak Ridge

Hickman, H. D.
Leed, R. E.
Zachry, D. S., Jr

Oak Ridge Gaseous Diffusion Plant

Wilcox, W. J., Jr
Winkel, R. A.

Oak Ridge Y-12 Plant

Alvey, H. E.
Burditt, R. B.
Briscoe, O. W.
Burkhart, L. E.
Butturini, W. G.
Duggan, H. G.
Ebert, J. W.
Ellingson, R. D.
Fraser, R. J.
Gambill, E. F.
Gritzner, V. B.
Hensley, C. E.
Johnson, C. E.
Kahl, K. G.
Keith, A.
King, A. (10)
McLendon, J.D.
Mills, J. M., Jr
Oliphant, G. W.
Perry, A. E.
Phillips, L. R.
Smith, H. F., Jr
Smith, R. D.
Snyder, H. G. P.
Weathersby, W. E.
West, C. M.
Whitson, W. K.
Yaggi, W. J./Googin, J. M.
Y-12 Central Files (5)
Y-12 Central Files (master copy)
Y-12 Central Files (route copy)
Y-12 Central Files (Y-12RC)
Zerby, C. D.

Paducah Gaseous Diffusion Plant

Edwards, A. K.

In addition, this report is distributed in accordance with the category UC-41, **Health and Safety**, as given in the *USERDA Standard Distribution Lists for Unclassified Scientific and Technical Reports*, TID-4500.